

New Evidence of the Azimuthal Alignment of Quasars Spin Vector in the LQG U1.28, U1.27, U1.11, Cosmologically Explained.

REINOUD J. SLAGTER¹

¹*Astronomisch Fysisch Onderzoek Nederland (ASFYON)*

and

University of Amsterdam (on leave)

1405EP Bussum, The Netherlands

Submitted to JCAP

ABSTRACT

There has been observational evidence about spin axes of quasars in large quasar groups correlated over hundreds of Mpc. This is seen in the radio spectrum as well as in the optical range. There is not yet a satisfactory explanation of this "spooky" alignment. This alignment cannot be explained by mutual interaction at the time that quasars manifest themselves optically. A cosmological explanation could be possible in the formation of superconducting vortices (cosmic strings) in the early universe, just after the symmetry-breaking phase of the universe. We gathered from the NASA/IPAC and SIMBAD extragalactic databases the right ascension, declination, inclination, position angle and eccentricity of the host galaxies of 3 large quasar groups to obtain the azimuthal and polar angle of the spin vectors. The alignment of the azimuthal angle of the spin vectors of quasars in their host galaxy is confirmed in the large quasar group U1.27 and compared with two other groups in the vicinity, i.e., U1.11 and U1.28, investigated by Clowes (2013). It is well possible that the azimuthal angle alignment fits the predicted azimuthal angle dependency in the theoretical model of the formation of general relativistic superconducting vortices, where the initial axially symmetry is broken just after the symmetry breaking of the scalar-gauge field.

Keywords: quasar groups – alignment spin vectors – host galaxy – cosmic strings – scalar-gauge field

1. INTRODUCTION

A large quasar group (LQG) is a cluster of quasars that makes the largest astronomical structures in the current universe. Their sizes can be of the order of hundreds of Mpc. Astronomers believe that a quasar is an active galactic nuclei (AGN) with a vibrant eruption of radiation both optical and in radio range originated by a spinning (Kerr-) black hole, surrounded by an accretion disk. According to Taylor and Jagannathan (Taylor & Jagannathan 2016), a LQG has an internal non-uniform distribution of spin vectors seen in the radio spectrum and the optical spectrum as observed by Hutsemekers et al. (Hutsemekers 2014). This coherence is mysterious and cannot be explained by mutual interaction at the time scale of primordial galaxies formation but rather by use of a more advanced method (Slagter 2018). In a recent study, Slagter (Slagter & Miedema 2021) found that the azimuthal angle of the spin vector of quasars in their host galaxies in six quasar groups, show preferred directions. This is demonstrated through an emergent azimuthal angle dependency of the general relativistic Nielsen-Olesen (NO) vortices at the point after the symmetry breaking at grand unified theory (GUT)-scale. This review focuses on three more other LQG, studied by Clowes (Clowes 2012, 2013).

2. RESULTS

From the NASA/IPAC extragalactic database and SIMBAD we extract for the three LQG U1.11, U1.27 and U.28 the right ascension, declination, inclination, position angle and eccentricity of the host galaxies. The 3-D orientation of the spin vectors can then be calculated (Pajowska 2019). In figure 1 and 2 we plotted the azimuthal angle. Without statistical analysis one can conclude that the preferred orientations are evident. In the case of LQG U1.27 (see table 1 and 2 for the data), we fitted two trigonometric functions on the distribution, which can theoretically be explained (section 3).

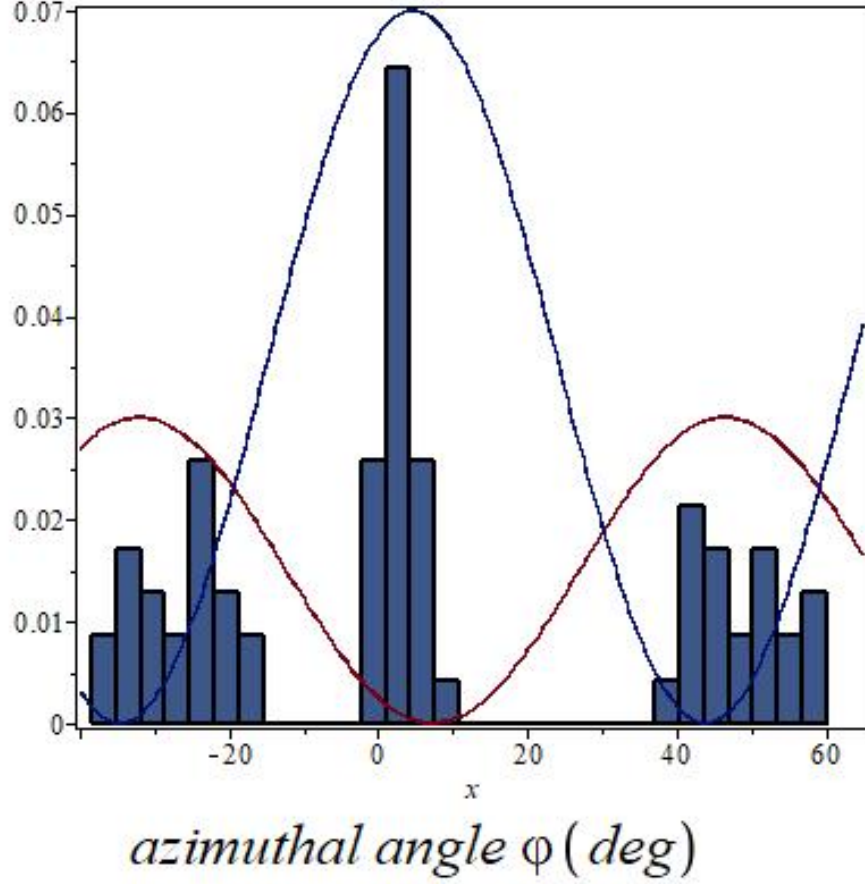


Figure 1. Plot of the azimuthal angle φ in degrees. This shows the distribution of the azimuthal angle of the spin vectors in the LQG U1.27 ($N=71$) with a best-fit of two trigonometric functions with a phase shift range of 45° .

3. THE THEORETICAL MODEL

A linear approximation of wavelike solutions of the Einstein equations is not adequate when one is dealing with high curvature (or high energy scale), i.e., close to the horizons of black holes or in the early stage of the universe at the time of mass formation by the Higgs mechanism. There will be a "back-reaction" on the background spacetime. There is a powerful approximation method which can deal with these non linearities: the multiple-scale method. Pioneer work was done by ChoquetBruhat (Choquet-Bruhat 1968). One expands the relevant fields (Slagter 1986)

$$V_i = \sum_{n=0}^{\infty} \frac{1}{\omega^n} F_i^{(n)}(\mathbf{x}, \xi), \quad (1)$$

where ω represents a dimensionless parameter ("frequency"), which will be large. Further, $\xi = \omega\Theta(\mathbf{x})$, with Θ a scalar (phase) function on the manifold. The small parameter $\frac{1}{\omega}$ can also be the ratio of the characteristic wavelength of the perturbation to the characteristic dimension of the background. On warped spacetimes it could also be the ratio of

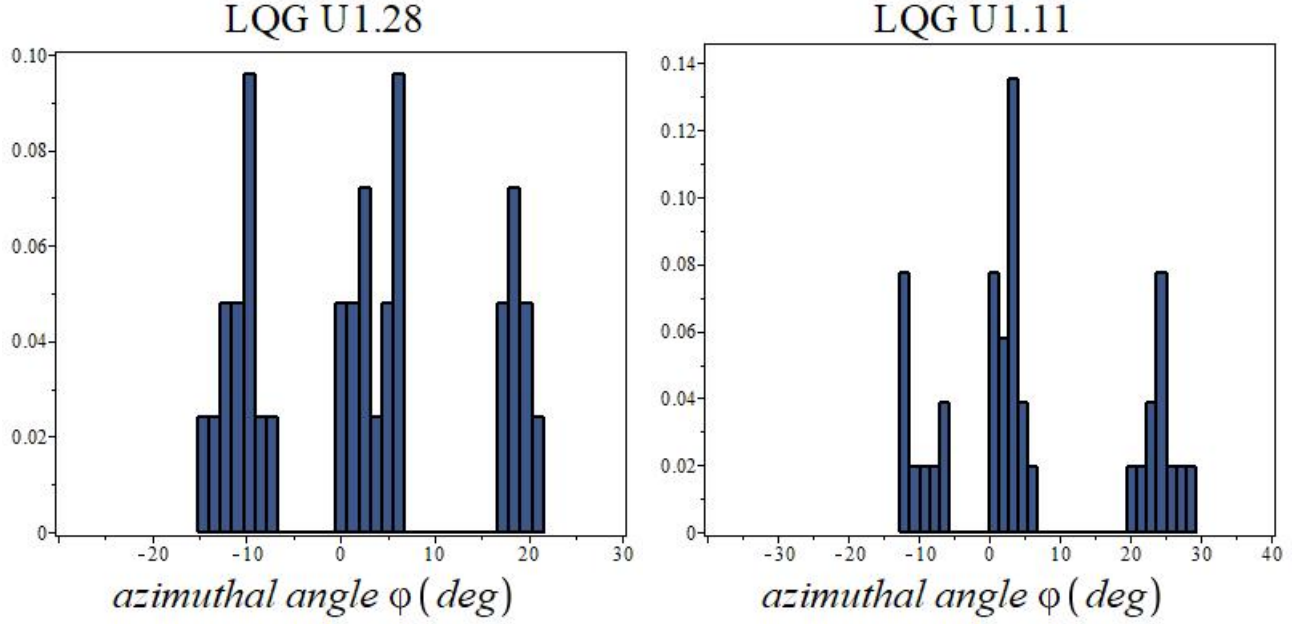


Figure 2. Plot showing the distribution of the azimuthal angle φ for the LQG U1.28 ($N=34$) and U1.11 ($N=38$).

the extra dimension to the background dimension. In the vacuum case, we expand the metric

$$g_{\mu\nu} = \bar{g}_{\mu\nu} + \frac{1}{\omega} h_{\mu\nu}(\mathbf{x}, \xi) + \frac{1}{\omega^2} k_{\mu\nu}(\mathbf{x}, \xi) + \dots, \quad (2)$$

where we defined

$$\frac{dg_{\mu\nu}}{dx^\sigma} = g_{\mu\nu,\sigma} + \omega l_\sigma \dot{g}_{\mu\nu}, \quad g_{\mu\nu,\sigma} = \frac{\partial g_{\mu\nu}}{\partial x^\sigma}, \quad \dot{g}_{\mu\nu} = \frac{\partial g_{\mu\nu}}{\partial \xi}, \quad (3)$$

with $l_\mu = \frac{\partial \Theta}{x^\mu}$. One then says that

$$V_i = \sum_{n=-m}^{\infty} \frac{1}{\omega^n} F_i^{(n)}(\mathbf{x}, \xi) \quad (4)$$

is an approximate wavelike solution of order n of the field equation, if $F_i^{(n)} = 0, \forall n$. One can substitute the expansion into the field equations. The Ricci tensor then expands as

$$R_{\mu\nu} \rightarrow \omega R_{\mu\nu}^{(-1)} + \left(\bar{R}_{\mu\nu} + R_{\mu\nu}^{(0)} \right) + \frac{1}{\omega} R_{\mu\nu}^{(1)} + \dots \quad (5)$$

By equating the subsequent orders to zero, we obtain

$$R_{\mu\nu}^{(-1)} = 0 = \frac{1}{2} \bar{g}^{\beta\lambda} (l_\lambda l_\mu \ddot{h}_{\beta\nu} + l_\nu l_\beta \ddot{h}_{\mu\lambda} - l_\lambda l_\beta \ddot{h}_{\mu\nu} - l_\nu l_\mu \ddot{h}_{\beta\lambda}), \quad (6)$$

$$R_{\mu\nu}^{(0)} + \bar{R}_{\mu\nu} = 0, \quad R_{\mu\nu}^{(1)} = 0, \quad \dots \quad (7)$$

Here we used $l_\mu l^\mu = 0$. The rapid variation is observed in the direction of l_μ . In the radiative outgoing Eddington-Finkelstein coordinates, we have $x^1 = u = \Theta(\mathbf{x}) = t - r$ and $l_\mu = (1, 0, 0, 0)$, while the bar stands for the background.

3.1. Formation of vortices

In a recent study (Slagter 2016, 2017; Slagter & Miedema 2021) we applied this non-linear approximation scheme on a FLRW spacetime. We considered the matter contribution of a gauged complex scalar (Higgs) field. Physicists

are now convinced that this field plays a fundamental role in the early universe and is responsible for the symmetry breaking in the Standard Model of particle physics. The experimental verification came by the recently observed Higgs particle at CERN. The same field has lived up to its reputation in superconductivity, where the field act as an order parameter to describe the formation of Cooper pairs. The scalar field is combined with a gauge field, parameterized as $\Phi = \eta X(\mathbf{x})e^{in\varphi}$ and $A_\mu(\mathbf{x}) = \frac{n}{e}(P(\mathbf{x}) - 1)\nabla_\mu\varphi$, with n the topological charge or winding number. The trapped flux of the vortex is expressed as $n\frac{2\pi\hbar}{e}$. The formation of a lattice of quantized magnetic flux tubes was first observed by Abrikosov (Abrikosov 1957) and are described by the famous equations of Ginzberg (Ginzberg & Landau 1950).

In these models, one needs the quartic potential of the Higgs field, i.e., $V(\Phi) = \frac{1}{8}\lambda(\Phi\Phi^* - \eta^2)^2$, with η the vacuum expectation value. Further, $\frac{m_\Phi}{m_A} = \frac{e^2}{\lambda}$ is the ratio of the scalar to gauge masses. This potential leads to a nonzero η and spontaneous breaking of the $U(1)$ symmetry (note that the parameters are in general temperature dependent). The forces existing between the vortices are the electromagnetic and scalar force. When the vortices get close together, the problem becomes non-linear and the resulting force depends on the ratio $\frac{e^2}{\lambda}$. For details, see, for example, the text books of Felsager (Felsager 1998) and Weinberg (Weinberg 2012). Moreover, when the vortices are formed in the early stage of the universe, then gravity will come into play. These general relativistic vortex solutions are known as "cosmic strings" (Garfinkle 1985; Vilenkin & Shellard 1994), when they extend to cosmological dimensions. They could possible explain the observed void and filament structures in the universe. We expand the scalar and gauge field to second order as

$$A_\mu = \bar{A}_\mu(\mathbf{x}) + \frac{1}{\omega}B_\mu(\mathbf{x}, \xi) + \frac{1}{\omega^2}C_\mu(\mathbf{x}, \xi) + \dots, \quad (8)$$

$$\Phi = \bar{\Phi}(\mathbf{x}) + \frac{1}{\omega}\Psi(\mathbf{x}, \xi) + \frac{1}{\omega^2}\Xi(\mathbf{x}, \xi) + \dots, \quad (9)$$

where we write the subsequent orders of the scalar field as

$$\bar{\Phi} = \eta\bar{X}(t, r)e^{in_1\varphi}, \quad \Psi = Y(t, r, \xi)e^{in_2\varphi}, \quad \Xi = Z(t, r, \xi)e^{in_3\varphi}, \quad (10)$$

with n_i the winding numbers.

3.2. The azimuthal angle dependency: breaking the axial symmetry

The azimuthal angle φ does not reach the partial differential equations (PDE) in the unperturbed case. By quantum fluctuations, the vortex excite in higher n -state and will dissociate into n well separated $n = 1$ vortices¹, because the energy of the configuration is proportional with n^2 . The topological characterization is a set of isolated points with winding numbers n_i (the zeros of Φ), with $n = n_1, n_2, \dots$. This n -vortices solution represents a finite energy configuration. However, an imprint will be left over of the azimuthal dependency of the orientation of the clustering of Abrikosov vortices lattice in the general relativistic situation. So the axial symmetry is dynamically broken. The azimuthal dependency emerge already to first order in the approximation. For example, the energy-momentum tensor $T_{t\varphi} = 0$, while the first order perturbation becomes

$$T_{t\varphi}^{(0)} = \bar{X}\bar{P}\dot{Y}n_1\sin(n_2 - n_1)\varphi \quad (11)$$

However, in $T_{t\varphi}^{(1)}$ there appears terms like $\cos(n_2 - n_1)\varphi$ and $\sin(n_3 - n_1)\varphi$. The perturbative appearance of a nonzero energy-momentum component $T_{t\varphi}$ can be compared with the phenomenon of bifurcation along the Maclaurin-Jacobi sequence of equilibrium ellipsoids of self-gravitating compact objects, signalling the onset of secular instabilities (Gondek-Rosinska & Gourgoulhon 2002). This shows a similarity with the Goldstone-boson modes of spontaneously broken symmetries of continuous groups. The recovery of the $SO(2)$ symmetry from the equatorial eccentricity takes place at a time comparable to the emission of gravitational waves.

The particular ellipsoid orientation in the frame (r, φ, z) expressed as $\varphi_0 \equiv \varphi(t_0)$, is at $t > t_0$ and determined by the transformation $\varphi \rightarrow \varphi_0 - Jt$, where J is the rotation frequency (circulation or "angular momentum") of the coordinate system. The angle φ_0 is fixed arbitrarily at the onset of symmetry breaking.

¹ The stability of the configuration depends on parameter λ (Weinberg 2012)

3.3. The pure gravitational radiation case

So far, we found that temporarily off-diagonal terms occurred in the perturbative approach of the Einstein scalar gauge field. What remains unclear is if the breaking of the axially symmetry already appears in the vacuum case like in the vicinity of the black hole spacetime. It is conjectured that the formation of primordial (Kerr-) black holes (and so quasars) happened in the early stages of the evolution of the universe before the stars were formed. Therefore, consider the radiative Vaidya spacetime in Eddington-Finkelstein coordinates ²

$$ds^2 = -\left(1 - \frac{2M(u)}{r}\right)du^2 - 2dudr + r^2(d\theta^2 + \sin^2\theta d\varphi^2), \quad (12)$$

which is the Schwarzschild black hole spacetime with $u = t - r - 2M \log(\frac{r}{2M} - 1)$. Here we used $l_\mu l^\mu = 0$. In the radiative coordinates, we have $x^1 = u = \Theta(\mathbf{x})$ and $l_\mu = (1, 0, 0, 0)$. From Eq.(6) we obtain

$$h_{rr} = h_{r\theta} = h_{r\varphi} = 0, \quad h_{\varphi\varphi} = -\sin^2\theta h_{\theta\theta} \quad (13)$$

From the zero-order equations Eq.(7) we obtain

$$\ddot{k}_{rr} = 0, \quad \dot{h}_{\theta\theta} = r\partial_r \dot{h}_{\theta\theta}, \quad \dot{h}_{\theta\varphi} = r\partial_r \dot{h}_{\theta\varphi}. \quad (14)$$

So one writes

$$h_{\theta\theta} = r\alpha(u, \theta, \varphi, \xi), \quad h_{\theta\varphi} = r\beta(u, \theta, \varphi, \xi), \quad h_{\varphi\varphi} = -r\alpha \sin^2\theta. \quad (15)$$

Further, we have

$$\ddot{k}_{r\theta} = \frac{1}{r} \left(2\dot{\alpha} \cot\theta + \partial_\theta \dot{\alpha} + \frac{1}{\sin^2\theta} \partial_\varphi \dot{\beta} \right), \quad (16)$$

$$\ddot{k}_{r\varphi} = \frac{1}{r} \left(\dot{\beta} \cot\theta - \partial_\varphi \dot{\alpha} + \partial_\theta \dot{\beta} \right), \quad (17)$$

$$\frac{dM}{du} = -\frac{\ddot{k}_{\phi\phi} + \sin^2\theta \ddot{k}_{\theta\theta}}{4\sin^2\theta} - \frac{1}{2} r \dot{h}_{uu} - \frac{1}{4} \left(\dot{\alpha}^2 + \frac{\dot{\beta}^2}{\sin^2\theta} \right) + \frac{1}{4} \left(\ddot{\alpha}^2 + \frac{\ddot{\beta}^2}{\sin^2\theta} \right). \quad (18)$$

Not all the components of $h_{\mu\nu}$ and $k_{\mu\nu}$ are physical, so one needs some extra gauge conditions. Suitable choice of α and β (Choquet-Bruhat uses, for example, $\alpha = 0, \beta = g(u)h(\xi)\sin\theta$), leads to a solution to second order which is in general not axially symmetric. We can integrate these zero order equations with respect to ξ . One obtains then some conditions on the background fields, because terms like $\int \dot{\alpha} d\xi$ disappear. From Eq.(18), we obtain

$$\frac{dM}{du} = -\frac{1}{4\tau} \int_0^\tau \left(\dot{\alpha}^2 + \frac{\dot{\beta}^2}{\sin^2\theta} \right) d\xi, \quad (19)$$

which is the back-reaction of the high-frequency disturbances on the mass M . τ is the period of $\dot{h}_{\mu\nu}$. This expression can be substituted back into Eq.(18). However, in the non-vacuum case, the right-hand side will also contain contributions from the matter fields. In order to obtain propagation equations for $h_{\mu\nu}$ and $k_{\mu\nu}$, one proceeds with the next order equation $R_{\mu\nu}^{(1)} = 0$. First of all, Eq.(16), (17) are consistent with $R_{r\varphi}^{(1)} = 0$ and $R_{r\theta}^{(1)} = 0$. Further, one obtains propagation equations for α and β and for some second order perturbations, such as $k_{\varphi\varphi}$. Moreover, the (φ, θ) -dependent part of the PDE's for α and β (say $A(\theta, \varphi), B(\theta, \varphi)$) can be separated (for the case $k_{\theta\varphi} \neq 0$):

$$\partial_\varphi B + 2\sin\theta \cos\theta A + \sin^2\theta \partial_\theta A = 0, \quad (20)$$

$$\sin^2\theta \partial_\theta \partial_\theta A + 7\sin\theta \cos\theta \partial_\theta A + 4\cot\theta \partial_\varphi B + 2(5\cos^2\theta - 1)A + 2\partial_\theta \varphi B = 0. \quad (21)$$

A non-trivial simple solution is

$$A = \frac{\cos\theta(\sin\varphi + \cos\varphi)}{\sin^3\theta}, \quad B = \frac{\sin\varphi - \cos\varphi}{\sin^2\theta} + G(\theta), \quad (22)$$

with $G(\theta)$ arbitrary. So the breaking of the spherically and axially symmetry is evident.

² This spacetime is also applied to describe the evaporation of a black hole by hawking radiation in a quantum mechanical way.

4. CONCLUSIONS

There is clear new observational evidence for the azimuthal alignment of the spin vectors of quasars in three new studied LQG. This research presents a new argument about the theoretical explanation of the axial symmetry breaking in a non-linear perturbation scheme considering a vacuum black hole spacetime in radiative coordinates. The recently discovered 13 billion years old quasar P172+18 powered by a supermassive black hole, is all the more reason to believe that the formation of these objects took place in the very early universe.

5. APPENDIX: THE DATA

The data of LQG U1.27 underlying this article are gathered in Table 1 and 2.

REFERENCES

- Abrikosov, A. A. 1957, *Sov. Phys. JETP*, 5, 1174
- Choquet-Bruhat, Y. 1968, *Commun. math. Phys.*, 12, 16
- Clowes, R. G. e. a. 2012, *Mon. Not. R. Astron. Soc.*, 419, 556
- Clowes, R. G. e. a. 2013, *Mon. Not. R. Astron. Soc.*, 429, 2910
- Felsager, B. 1998, *Geometry, Particles and Fields* (Odense Univ. Press, Odense)
- Garfinkle, D. 1985, *Phys. Rev. D*, 32, 1323
- Ginzberg, V. L. & Landau, L. D. 1950, *Zh.Eksp.Teor.Fiz.*, 20,1064
- Gondek-Rosinska, D. &ourgoulhon, E. 2002, *Phys. Rev. D*, 66, 044021
- Hutsemekers, D., e. a. 2014, *A&A*, 572, A18
- Pajowska, P., e. a. 2019, *J. Cosm. Astroparticles*, 02, 005
- Slagter, R. J. 1986, *Astrophys. J.*, 307, 20
- Slagter, R. J. 2016, *Journal of Modern Physics*, 08, 163
- Slagter, R. J. 2017, *Journal of Modern Physics*, 08, 163
- Slagter, R. J. 2018, *Int. J. Mod. Phys. D*, 27, 1850094
- Slagter, R. J. & Miedema, P. G. 2021, *Mon. Not. Roy. Astron. Soc.*, 501, 3054
- Taylor, A. R. & Jagannathan, P. 2016, *Mon. Not. R. Astron. Soc.*, 459, L36
- Vilenkin, A. & Shellard, E. P. S. 1994, *Cosmic Strings and Other Topological Defects* (Cambridge Univ. Press, Cambridge)
- Weinberg, E. J. 2012, *Classical Solutions in Quantum Field Theory* (Cambridge Univ. Press, Cambridge)

Table 1. Data for the LQG U1.27 (N=71) from NASA/IPAC and SIMBAD. The successive columns represent: right ascension, declination, redshift, inclination, eccentricity, position angle, azimuthal angle and polar angle.

U1.27	RA	Dec	z	inc	ecc	PA(deg)	$\varphi(\text{rad})$	$\theta(\text{rad})$
1	160.413150	14.591740	1.221	.830	.69	87	$\pm.298 / \pm.427$	$.575 (\pi-.575) / 1.083 (\pi-1.083)$
2	160.840103	14.600057	1.271	.606	.83	113	$.571 / .013$	$.305 / .796$
3	161.128848	16.045854	1.233	.526	.87	45	$.034 / .782$	$.619 / .102$
4	161.187666	15.317133	1.237	.741	.75	68	$.049 / .763$	$.421 / .925$
5	161.335962	14.290068	1.270	.586	.84	63	$.063 / .678$	$.751 / .275$
6	161.516893	14.044789	1.290	.547	.86	6	$.227 / .889$	$-.155 / .263$
7	161.567993	16.753510	1.282	.772	.73	48	$.186 / 1.04$	$.779 / .294$
8	161.601093	14.502540	1.372	.660	.80	60	$.007 / .775$	$.322 / .792$
9	162.056815	16.480304	1.290	.506	.88	170	$.82 / .215$	$.336 / -.167$
10	162.248981	12.889527	1.368	.677	.79	99	$.419 / .156$	$.434 / .890$
11	162.344193	15.726700	1.263	.772	.73	42	$.257 / 1.05$	$.258 / .699$
12	162.351272	15.698897	1.301	.435	.91	8	$.129 / .762$	$-.190 / .306$
13	162.409269	21.808144	1.235	.526	.87	33	$.127 / .849$	$-.067 / .612$
14	162.423677	15.306867	1.341	.676	.79	3	$.379 / 1.00$	$-.175 / .240$
15	162.449082	16.371282	1.300	.566	.85	142	$.745 / .225$	$.080 / .589$
16	162.505093	15.565017	1.255	.357	.94	17	$.038 / .671$	$-.154 / .357$
17	162.676146	16.015594	1.269	.771	.73	125	$.744 / .340$	$.843 / .359$
18	162.767371	16.316926	1.253	.287	.96	170	$.592 / .004$	$.322 / -.224$
19	162.820881	13.193341	1.337	.483	.89	102	$.400 / .175$	$.700 / .243$
20	162.831696	14.436524	1.315	.659	.80	54	$.084 / .812$	$.743 / .287$
21	162.845783	11.981222	1.309	.437	.91	159	$.707 / .132$	$.344 / -.039$
22	162.857213	12.796204	1.283	.641	.81	139	$.779 / .275$	$.595 / .207$
23	162.884258	14.937553	1.367	.756	.74	94	$.354 / .211$	$1.014 / .494$
24	162.918357	20.655882	1.174	.567	.85	49	$.062 / .799$	$.743 / .082$
25	162.937035	12.974699	1.316	.461	.90	110	$.455 / .107$	$.654 / .207$
26	163.041780	16.928818	1.339	.436	.91	59	$.077 / .576$	$.656 / .083$
27	163.092251	12.515036	1.316	.355	.94	21	$.035 / .647$	$-.082 / .331$
28	163.098712	14.090468	1.256	.622	.82	101	$.415 / .127$	$.365 / .852$
29	163.100377	20.776172	1.203	.504	.88	25	$.160 / .827$	$-.120 / .525$
30	163.190868	13.682636	1.356	.482	.89	60	$.057 / .590$	$.181 / .643$
31	163.238226	10.992647	1.266	.483	.89	89	$.285 / .305$	$.291 / .674$
32	163.242363	20.284854	1.253	.356	.94	41	$.026 / .611$	$-.111 / .569$
33	163.552829	14.959790	1.231	.678	.79	120	$.625 / .184$	$.330 / .812$
34	163.591268	21.358676	1.257	.606	.83	120	$.579 / .164$	$.161 / .862$
35	163.648532	10.304548	1.260	.385	.93	16	$.084 / .671$	$-.064 / .271$
36	163.677979	10.722398	1.335	.725	.76	144	$.872 / .393$	$.247 / .550$
37	163.694730	19.952953	1.220	.566	.85	20	$.246 / .889$	$-.116 / .478$
38	163.845984	13.102997	1.358	.588	.84	11	$.295 / .889$	$.296 / -.085$
39	163.854942	19.298998	1.201	.773	.73	146	$.906 / .531$	$.651 / .133$
40	163.857047	11.617507	1.293	.527	.87	119	$.538 / .027$	$.650 / .260$

Table 2. continue

cont.	RA	Dec	z	inc	ecc	PA(deg)	φ (rad)	θ (rad)
41	163.924334	11.298387	1.331	.845	.68	88	.249 / .335	.648 / 1.042
42	163.984288	18.788475	1.277	.355	.94	87	.262 / .305	.027 / .683
43	164.046989	17.140997	1.344	.845	.68	72	.012 / .780	.505 / 1.066
44	164.091276	14.566966	1.243	.207	.98	129	.409 / .138	.412 / -.091
45	164.156218	15.013202	1.371	.787	.72	109	.541 / .147	.979 / .483
46	164.158278	10.052025	1.273	.435	.91	128	.544 / .023	.507 / .170
47	164.230688	14.829509	1.229	.625	.82	133	.696 / .257	.208 / .671
48	164.308435	18.798158	1.285	.382	.91	152	.614 / .106	-.133 / .484
49	164.521231	20.061417	1.273	.587	.94	72	.095 / .549	.211 / .895
50	164.633396	17.082247	1.286	.462	.90	17	.175 / .750	-.139 / .398
51	164.668752	17.904320	1.269	.527	.87	50	.062 / .700	.101 / .684
52	164.730550	8.230752	1.246	.677	.79	8	.401 / .953	-.025 / .199
53	164.869078	16.782794	1.300	.623	.82	116	.533 / .122	.272 / .829
54	165.025092	9.444098	1.252	.567	.85	65	.019 / .556	.348 / .666
55	165.070384	19.606880	1.240	.832	.69	114	.597 / .372	.423 / 1.040
56	165.166670	16.952878	1.300	.802	.71	127	.739 / .454	.354 / .851
57	165.452792	8.368669	1.196	.413	.92	9	.153 / .671	-.071 / .197
58	165.676652	8.655867	1.240	.411	.92	60	.046 / .481	.205 / .500
59	166.268588	8.759810	1.241	.566	.85	57	.072 / .606	.322 / .610
60	166.589189	8.686458	1.244	.548	.86	53	.098 / .618	.286 / .571
61	166.902560	9.020778	1.228	1.02	.55	87	.161 / .347	.860 / 1.175
62	166.935900	9.924171	1.225	.383	.93	14	.143 / .613	-.071 / .251
63	167.532914	10.802888	1.211	.248	.97	129	.374 / .052	.006 / .378
64	167.539961	7.868564	1.208	.740	.75	10	.508 / .967	.015 / .219
65	168.567405	10.390996	1.210	.693	.78	151	.803 / .472	.168 / .460
66	168.938775	8.249943	1.194	.547	.86	106	.349 / .012	.381 / .665
67	169.508801	10.550690	1.215	.526	.87	134	.548 / .234	.196 / .540
68	169.596744	9.084715	1.197	.787	.72	98	.303 / .018	.620 / .934
69	170.081761	8.984773	1.229	.641	.81	56	.193 / .613	.373 / .662
70	170.246993	10.185907	1.208	.384	.93	77	.085 / .271	.196 / .551
71	170.290711	7.999635	1.141	.461	.90	93	.195 / .143	.320 / .599